

carbonyl is approximately 36 kcal/mol.<sup>28</sup> Using these numbers and average values for the dissociation energy of subsequent carbonyls,<sup>32</sup> we are able to estimate which fragments could be the result of one-photon excitation of the parent molecule, based on energetic considerations. These fragments are marked with a check in Tables I and II. We also estimate that at all photolysis energies used a large amount of excess energy is deposited in the primary fragments.

$\text{Mn}_2(\text{CO})_{10}$  provides an ideal system in which to explore the competition between metal-metal and metal-CO bond reactivity in the excited electronic state. Excitation of the allowed  $\sigma \rightarrow \sigma^*$  transition reduces the formal metal-metal bond order from 1 to 0. Accordingly, earlier condensed-phase photochemical data indicated clean, efficient homolytic cleavage to 17 electron  $\text{Mn}(\text{CO})_5$  radicals.<sup>7,21-23</sup> Modern condensed-phase studies<sup>8,9a,14,24</sup> have since established a more complex photochemical pathway for  $\text{Mn}_2(\text{CO})_{10}$  in this electronic state. It involves two primary photoproducts, due to Mn-Mn bond homolysis and to CO loss, whose relative yields are sensitive to environmental effects. Experiments designed to explore the photochemical properties of this molecule in gas phase, in the absence of solvent cage effects, are currently in progress.<sup>17,20</sup>

The results reported here establish directly the nature of photoproducts generated on excitation of  $\text{Mn}_2(\text{CO})_{10}$  into the  $\sigma^*$  state using 350-nm photons. Approximately equal amounts of  $\text{Mn}_2(\text{CO})_8^+$  and  $\text{Mn}(\text{CO})_5^+$  are generated on photolysis at this energy. These results are obtained at the lowest laser flux at which signal can be obtained in our instrument. The relative intensities and extent of fragmentation are extremely dependent on laser flux. At higher laser fluxes multiphoton processes become important and highly dissociated fragments, such as  $\text{Mn}^+$ ,  $\text{Mn}_2^+$ ,  $\text{Mn}(\text{CO})^+$ , and  $\text{Mn}_2(\text{CO})_3^+$ , dominate the spectrum. This extreme depen-

dence on laser flux makes this system difficult to study by less direct techniques.

The results presented establishing the existence of two gas-phase photochemical pathways, metal bond homolysis and CO loss, agree well with results obtained spectroscopically using time-resolved IR absorption and MPI techniques.<sup>17,20</sup> The photochemistry of the  $S_1$  state of  $\text{Mn}_2(\text{CO})_{10}$  in the gas phase is found to be consistent with that of the molecule in solution.<sup>14,24</sup>

The energy dependence of the photochemistry of this molecule is investigated by excitation of the  $\pi^*$  state. At 248 nm ( $d\pi \rightarrow \pi^*$  transition) the primary photofragment detected is  $\text{Mn}_2(\text{CO})_9$ , with no detectable metal bond homolysis products. The trend continues as excitation at 193 nm ( $M \rightarrow \pi^*$  transition) yields only  $\text{Mn}_2(\text{CO})_5$ . This fragment is presumably formed by CO loss from the initially formed, highly excited  $\text{Mn}_2(\text{CO})_9$ .

The energy dependence of the photochemistry of  $\text{Mn}_2(\text{CO})_{10}$  is consistent both with the conclusions of time-resolved gas-phase studies and time-resolved experiments in solution.<sup>14,20,24</sup>

### Conclusion

The photochemistry of  $\text{Mn}_2(\text{CO})_{10}$  in the gas phase is investigated with a direct experiment based on mass spectroscopic detection of primary photofragments. The results indicate that excitation of the  $\sigma^*$  state leads to both metal bond homolysis and ligand loss. Excitation of the  $\pi^*$  state leads to ligand loss. These results agree with recent studies of the photochemistry of this molecule both in gas and condensed phases. The extensive information now available establishes  $\text{Mn}_2(\text{CO})_{10}$  as the first transition metal cluster complex for which a comprehensive picture of the chemistry of the electronic states is available.

**Acknowledgment.** Financial support from the National Science Foundation (Grant No. CHE-8607697) is gratefully acknowledged. We wish to thank Professor E. Weitz for making their data on  $\text{Mn}_2(\text{CO})_{10}$  available to us prior to its publication.

(32) Svec, H. J.; Junk, G. A. *J. Am. Chem. Soc.* 1967, 89, 2836.

## The Structure of the Methylnitrene Radical

P. G. Carrick,<sup>1a</sup> C. R. Brazier,<sup>1b</sup> P. F. Bernath,<sup>\*1b</sup> and P. C. Engelking<sup>\*1c</sup>

Contribution from the Department of Physics, Mississippi State University, Mississippi State, Mississippi 39762, Department of Chemistry, University of Arizona, Tucson, Arizona 85721, and Department of Chemistry, University of Oregon, Eugene, Oregon 97403.

Received February 6, 1987

**Abstract:** The geometry and electronic spin-spin splitting have been determined for the methylnitrene radical by high-resolution gas-phase emission spectroscopy of the  $\tilde{A}^3E-\tilde{X}^3A_2$  transition. The equivalent of the ESR  $D$  constant is  $1.720 \pm 0.004 \text{ cm}^{-1}$ , significantly larger than the previously attributed value. The ground state C-N single bond ( $1.411 \pm 0.001 \text{ \AA}$ ) is noticeably shorter than that found in calculations on this radical or in other compounds containing a C-N single bond.

Methylnitrene ( $\text{CH}_3\text{N}$ , methylimidogen) introduces the series of alkylnitrene radicals. Small enough to allow good theoretical and experimental treatments, it provides numerous tests of our current understanding of the structure of nitrene radicals. Here we present the structure of methylnitrene as revealed by high resolution UV spectroscopy.

Two factors may complicate the electronic structure of the open-shell nitrene radical. First, the vacancies in the valence shell, formally localized in nonbonding p-orbitals on the nitrogen, may "delocalize", spreading toward the alkyl end of the radical. This would modify directly the H-C bonding and may add double bond character to the C-N bond. Second, the open-shell nitrogen may

take advantage of having to attend to only one bond and adjust its own electronic structure to optimize this C-N bond. This would show up in an anomalous C-N single bond and possibly may modify the H-C bonding by changing the electronic structure at the carbon.

Calculations<sup>2-4</sup> indicate that the ground state of the nitrene radical is a triplet electronic state,  $^3A_2$ . Two electronic singlets

(2) (a) Yarkony, D. R.; Schaefer, H. F., III; Rothberg, S.; *J. Am. Chem. Soc.* 1974, 96, 5974. (b) Demuyneck, J.; Fox, D. J.; Yamaguchi, Y.; Schaefer, H. F., III. *J. Am. Chem. Soc.* 1980, 102, 6204.

(3) (a) Lathan, W. A.; Curtiss, L. A.; Hehre, W. J.; Lisle, J. B.; Pople, J. A. *Prog. Phys. Org. Chem.* 1974, 11, 175. (b) Pople, J. A.; Raghavachar, K.; Frisch, M. J.; Binkley, J. S.; Schleyer, P. v. *J. Am. Chem. Soc.* 1983, 105, 6389.

(4) Ha, T. K.; Nguyen, M. T. *THEOCHEM.* 1982, 4, 355.

(1) (a) Mississippi State University. (b) University of Arizona. (c) University of Oregon.

lie directly above this state, and there is a higher lying triplet of symmetry  ${}^3E$ . The C–N bond lengths in the triplet ground state are generally calculated to be the same as, or longer than, the C–N single bond in methylamine. The notable exception is the recent calculation of Pople and co-workers,<sup>3b</sup> who find a C–N bond shorter than that found by previous workers. The bond angles of the hydrogens are generally found to be at, or near, tetrahedral angles. Overall, the picture that emerges from current calculations is one of a radical that has bond lengths and angles similar to those of analogous closed shell molecules.

It should be expected that the geometry of methylnitrene determined experimentally would reflect the results of current calculations, and it would have structural constants very similar to those of methylamine. An experimental test of the nitrene ground state would, on the one hand, indicate how important delocalization and single bond optimization effects are in the radical, while, on the other hand, would indicate how well understood these systems are theoretically.

Additional information on nitrene radicals comes from ESR spectra. Since the ground-state radical is a triplet, a characteristic electronic spin–spin splitting should be found for alkylnitrenes. The characteristic value for this is thought to be between 1 and 2  $\text{cm}^{-1}$ . An early report gave this as  $D = 1.595 \text{ cm}^{-1}$  for methylnitrene;<sup>5</sup> however, this is questionable on several grounds.<sup>6</sup> Recent work<sup>7,8</sup> on norbornyl- and adamantylnitrenes finds for these species values near 1.65  $\text{cm}^{-1}$ . For ESR work, it is important to have clear expectations for the values of  $D$  for methyl- and other alkylnitrenes. Thus, independent measurements of the electronic spin–spin interaction are valuable.

The geometry and electronic spin–spin couplings can be obtained from a rotational analysis of an electronic transition of methylnitrene. Vibrational bands of a UV transition of methylnitrene have been observed in matrices<sup>6</sup> and in the gas phase.<sup>9,10</sup> We are currently analyzing the rotational structure of the  $\tilde{A}{}^3E$ – $\tilde{X}{}^3A_2$  transition of the simplest of alkylnitrenes. Already, we have determined the electronic spin–spin coupling, allowing us to comment in general on the ESR zero-field spin-splitting parameter  $D$  to be expected for alkylnitrenes. In particular, the matrix ESR signal previously ascribed to  $\text{CH}_3\text{N}$  appears to be that of another species. We also point out the unusually short C–N single bond.

## Experimental Section

Methylnitrene was prepared from methylazide in a nozzle expansion as previously described.<sup>10</sup> Emission spectra of the rotationally cold radicals were taken with the McMath Fourier transform spectrometer at the National Solar Observatory at Kitt Peak.

Additional spectra have been taken by using ultraviolet laser excitation spectroscopy. Spin-orbit cooling of the  ${}^3E$  excited state produces jet-cooled emission spectra with only the lowest spin-orbit component  ${}^3E_2$  present in appreciable intensity. To facilitate assignment of the remaining two spin-orbit states, laser excitation spectra were obtained by using intercavity doubling of a CW ring dye laser (Coherent Model 699–29).

The methylnitrene radical is a triplet prolate symmetric top rotor with expected rotational constants of  $A = 5 \text{ cm}^{-1}$  and  $B = 1 \text{ cm}^{-1}$ . The perpendicular  ${}^3E$ – ${}^3A_2$  transition should result in a series of  $\Delta K = \pm 1$  sub-bands for each set of  $J$  levels. Energy and nuclear spin statistics for  $\text{CH}_3\text{N}$  should result in different intensities for these sub-bands, with  $K' = 1 \rightarrow K'' = 0$  much stronger than the other sub-bands.<sup>11</sup> The strongest sub-band (assigned to  $K' = 1 \rightarrow K'' = 0$ ) has been analyzed by the simple  ${}^3\Pi$ – ${}^3\Sigma^-$  Hamiltonian originally used in the analysis of the same transition

Table I. Rotational Constants<sup>c</sup>

constant	$\text{CH}_3\text{N}$	$\text{CD}_3\text{N}$
$B''$	0.93084 (18)	0.74410 (18)
$\lambda''$	0.8601 (23)	0.8572 (28)
$\gamma''$		–0.00411 (51)
$T_0$	31823.9149 (74)	31774.1584 (23) <sup>a</sup>
$B'$	0.84550 (28)	0.69060 (19)
$\lambda'$	–0.1986 (27)	<i>b</i>
$\gamma'$	0.0499 (40)	<i>b</i>
$A$	–22.8722 (69)	–22.87 <sup>a,b</sup>
<i>o</i>	1.8420 (46)	<i>b</i>
<i>q</i>	–0.00388 (56)	<i>b</i>

<sup>a</sup> Calculated assuming  $A(\text{CH}_3\text{N}) = A(\text{CD}_3\text{N})$ . <sup>b</sup> These parameters cannot be determined from the  ${}^3E_2$  spin component. The  ${}^3E_1$  and  ${}^3E_0$  components of the  $\tilde{A}$  state were not observed in the Fourier transform emission spectrum. <sup>c</sup> Calculated from a fit of 86 transitions with a standard deviation of 0.008  $\text{cm}^{-1}$ . All values are in  $\text{cm}^{-1}$ ; uncertainties of 1 standard deviation in the last two digits are given in parentheses.

Table II. Structure of  $\text{CH}_3\text{N}^f$

state	$R_{\text{CN}}$ (Å)	$\theta_{\text{HCH}}$ (deg)
$\tilde{X}{}^3A_2$	1.4106 (09)	106.68 (73) <sup>a</sup>
Schaefer <sup>b</sup>	1.471	109
Pople <sup>c</sup>	1.433	
Nguyen <sup>d</sup>	1.497	109
$\text{CH}_3\text{NH}_2^e$	1.474	109.47 (50)
$\tilde{A}{}^3E$	1.5136 (11)	111.72 (63)

<sup>a</sup> Uncertainties calculated include an uncertainty of 0.01 Å for the CH bond length. <sup>b</sup> Reference 2. <sup>c</sup> Reference 3b. <sup>d</sup> Reference 4. <sup>e</sup> Reference 16. <sup>f</sup> Calculated from the constants in Table I. The CH bond length was fixed at 1.09 Å. Uncertainties in the last two digits are given in parentheses.

in  $\text{NH}$ .<sup>12</sup> The resulting assignment accounts for approximately one-third of the observed rotational lines for the vibrational origin band transition but is adequate for determination of the geometry as presented here. A full analysis is being conducted to produce a complete characterization of all the observed sub-bands of the origin vibrational band and those of additional vibrational bands; however, the final fit of the spectrum is not expected to change the geometries as derived here.

## Results

For the determination of the geometry of methylnitrene, the important constants are the values of  $B$  determined for both protonated and deuterated radicals. The Fourier transform emission data, combined with 21 laser observations, resulted in a least-squares fit of 86 rotational transitions, including data from all three spin-orbit components, of the origin band. The rotational constants obtained from this fit are presented in Table I. The  $T_0$  value for  $\text{CD}_3\text{N}$  was calculated assuming a spin-orbit splitting of 22.87  $\text{cm}^{-1}$ , since laser data for the unobserved spin components of  $\text{CD}_3\text{N}$  are not available.

The constants listed in Table I were used to calculate the structure of the methylnitrene radical. Since only one  $K$  sub-band has been analyzed to date, the  $A$  rotational constant is undetermined. To calculate the structure of methylnitrene, it was therefore necessary to assume a constant CH bond length of 1.09 Å. The calculated structure is listed in Table II.

## Discussion

**ESR  $D$  Constant.** Methylnitrene has a  ${}^3A_2$  ground state. The unit electronic spin can form three projection states along the molecular axis:  $-1, 0, +1$ . In the nonrotating molecule, the  $\pm 1$  components are degenerate and are separate in energy from the 0 component by the zero-field spin–spin splitting constant. In gas-phase work we denote this as  $2\lambda$ ; in ESR work it is denoted  $D$ .<sup>14</sup> Our determination of the gas-phase  $\lambda = 0.860 \pm 0.002 \text{ cm}^{-1}$  allows us to predict the value to be expected for methylnitrene ESR spectra:  $D = 1.720 \pm 0.004 \text{ cm}^{-1}$ .

(5) (a) Barash, L.; Wasserman, E.; Jager, W. A. *J. Am. Chem. Soc.* **1967**, *89*, 3931. (b) Wasserman, E. *Prog. Phys. Org. Chem.* **1971**, *8*, 319.

(6) Ferrante, R. F. *J. Chem. Phys.* **1987**, *86*, 25.

(7) (a) Radziszewski, J. G.; Downing, J. W.; Wentrup, C.; Kaszynski, P.; Jawdosiuk, M.; Kovacic, P.; Michl, J. *J. Am. Chem. Soc.* **1984**, *106*, 7996. (b) Radziszewski, J. G.; Downing, J. W.; Kaszynski, P.; Jawdosiuk, M.; Kovacic, P.; Michl, J. *J. Am. Chem. Soc.* **1985**, *107*, 594.

(8) Radziszewski, J. G.; Downing, J. W.; Wentrup, C.; Kaszynski, P.; Jawdosiuk, M.; Kovacic, P.; Michl, J. *J. Am. Chem. Soc.* **1985**, *107*, 2799.

(9) Franken, T.; Perner, D.; Bosnali, M. W. *Z. Naturforsch., A: Astrophys., Phys., Phys. Chem.* **1970**, *25A*, 151.

(10) Carrick, P. G.; Engelking, P. C. *J. Chem. Phys.* **1984**, *81*, 1661.

(11) Herzberg, G. *Electronic Spectra of Polyatomic Molecules*; Van Nostrand Reinhold: New York, 1966.

(12) Brazier, C. R.; Ram, R. S.; Bernath, P. F. *J. Mol. Spectrosc.* **1986**, *120*, 381.

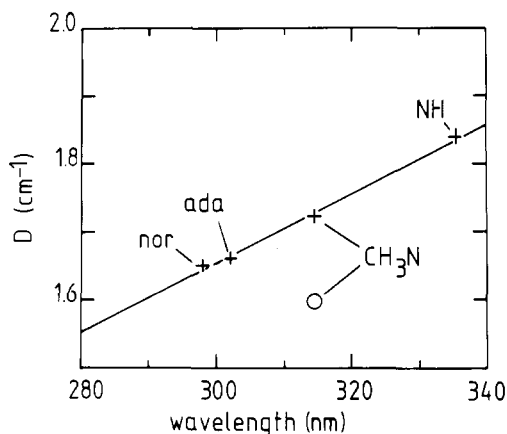


**Figure 1.** Relationship of the ESR splitting constant  $D$  to the wavelength of the  $\tilde{A}-\tilde{X}$  UV transition for several nitrenes. NH results are from ref 12, 14, and 15; adamantylnitrene (ada) and norbornylnitrene (nor) results are from ref 7 and 8. The previous ESR  $D$  value attributed to methylnitrene in ref 5 is shown with an open circle.

The  $D$  parameter is a sum of several interactions, including a direct spin-spin term, and an indirect term acting through higher energy states.<sup>13-15</sup> Thus, part of the splitting depends inversely upon the energy of the nearby electronic states, especially the  $\tilde{A}^3E$ . For several alkylnitrenes<sup>7,8</sup> and NH<sup>12,15</sup> for which both  $D$  and the equivalent of the  $\tilde{A}^3E$  electronic transition energy have been determined, an excellent correlation is found (Figure 1).

Note that the gas-phase value for methylnitrene falls upon the trend, while the previous ESR assignment<sup>5</sup> falls badly off the trend. Figure 1 suggests the ESR  $D$  parameters and  $\tilde{A}^3E-\tilde{X}^3A_2$  wavelengths to be expected for as yet unobserved alkylnitrenes.

**Geometry.** Our previous vibrational study,<sup>10</sup> the early gas-phase study,<sup>9</sup> and the recent matrix study<sup>6</sup> all point to a large change in the C-N bond length between the ground and excited states. The direction of the change toward a longer bond in the  $\tilde{A}$  state is indicated by the decrease in the C-N stretch vibrational frequency from 1039  $\text{cm}^{-1}$  in the  $\tilde{X}^3A_2$  state to 758  $\text{cm}^{-1}$  in the  $\tilde{A}^3E$  state. This large change is confirmed in the C-N bond lengths in Table II.

Our studies include deuteration at all hydrogen positions of  $\text{CH}_3\text{N}$ , giving two respective rotational  $B$  constants. Fixing the C-H bond length at  $1.09 \pm 0.01$  Å determines the HCH bond angle and the C-N bond length for the vibrationally averaged geometry. The derived HCH bond angle is sensitive to the assumed C-H bond length, but the derived C-N bond length is quite insensitive to assumptions about the C-H bond length. The C-N bond,  $r_{\text{CN}} = 1.411 \pm 0.001$  Å, is dramatically shorter than C-N single bonds in closed shell, fully bonded nitrogen compounds (e.g.,  $r_{\text{CN}} = 1.474$  Å in methylamine<sup>16</sup>). A bond this short has not been found in calculations on this radical (1.471,<sup>2</sup> 1.508,<sup>3a</sup> 1.433,<sup>3b</sup> and

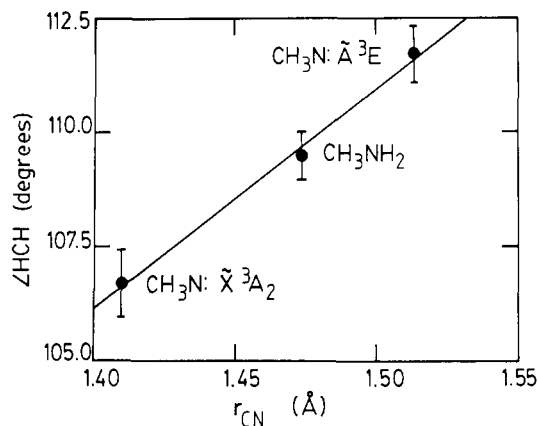


**Figure 2.** HCH bond angles and CN single bond lengths for methylnitrene ground state ( $\tilde{X}^3A_2$ ), excited state ( $\tilde{A}^3E$ ), and methylamine. Uncertainty in the CH bond length, taken as 1.09 Å in all three cases, is the major cause of uncertainty in the angle. Methylamine results are from ref 16.

1.497<sup>4</sup> Å). Thus, we have little guidance from calculations yet as to why the bond of a lone nitrogen to carbon should be shorter than in an amine.

The unusual bonding at the carbon is also reflected in the hydrogen bond angles. The hydrogens are farther away from the nitrogen in the radical than in methylnitrene, as shown by the bond angle ( $\angle\text{HCH} = 106.7 \pm 0.7^\circ$  in the radical compared with  $109.5^\circ$  in the amine). Regardless of the assumed H-C bond length, the plane of the three hydrogens lies at a greater distance from the nitrogen in the ground-state radical than in the corresponding amine. The HCH bond angle appears to be related to the strength of the C-N bond. In the excited  $\tilde{A}$  state, with the longer C-N bond, the HCH angle opens up. This leads to the correlation shown in Figure 2. The anomalously tight HCH angle in methylnitrene ground state has not yet been found in calculations, where the angle on carbon is either found or assumed to be tetrahedral.<sup>2-4</sup>

It should also be pointed out that bonding of other lone heteroatoms to a methyl leads to other anomalously short bonds: the C-O bond in methoxy is 0.049 Å shorter than in methanol, and the C-S bond in thiomethoxy is 0.023 Å shorter than in thiomethanol.<sup>17,18</sup>

**Acknowledgment.** We acknowledge Jeremy Wagner and Greg Ladd of the National Solar Observatory for assistance in acquiring this data. The National Solar Observatory is operated by the Association of Universities for Research in Astronomy, Inc. under contract with the National Science Foundation. Acknowledgment is made to the donors of the Petroleum Research Fund, administered by the ACS, for partial support of this work. This work was also supported by funding from the Office of Naval Research.

**Registry No.**  $\text{CH}_3\text{N}$ , 27770-42-9;  $\text{CD}_3\text{N}$ , 27770-43-0;  $\text{CH}_3\text{N}_3$ , 624-90-8.

(13) Kayama, K.; Baird, J. C. *J. Chem. Phys.* **1967**, *46*, 2604.

(14) Palmiere, P.; Sink, M. L. *J. Chem. Phys.* **1976**, *65*, 3641.

(15) Wayne, F. D.; Radford, H. G. *Mol. Phys.* **1976**, *32*, 1407.

(16) (a) Weast, R. C. *CRC Handbook of Chemistry and Physics*, 59th ed.; CRC Press: Boca Raton, FL, 1979; p 218. (b) Lide, D. R., Jr. *J. Chem. Phys.* **1957**, *27*, 343.

(17) Endo, Y.; Saito, S.; Hirota, E. *J. Chem. Phys.* **1984**, *81*, 122.

(18) Endo, Y.; Saito, S.; Hirota, E. *J. Chem. Phys.* **1986**, *85*, 1770.